Title
THE SELF-POTENTIAL METHOD IN GEOTHERMAL EXPLORATION

Author
Corwin, R.F.

Publication Date
1978-05-01

Submitted to Geophysics

LBL-7075 c.2
Preprint

THE SELF-POTENTIAL METHOD IN GEOTHERMAL EXPLORATION

Robert F. Corwin and Donald B. Hoover

May 1978

Prepared for the U. S. Department of Energy
under Contract W-7405-ENG-48

DISCLAIMER

The Self-Potential Method in Geothermal Exploration

Robert F. Corwin

Engineering Geoscience, University of California, Berkeley, CA

Donald B. Hoover

U.S. Geological Survey, Denver, Colorado

May, 1978

Table of Contents

ABSTRACT

Laboratory measurements and field data indicate that self-potential anomalies comparable to those observed in many areas of geothermal activity may be generated by thermoelectric or electrokinetic coupling processes. A study using an analytical technique based on concepts of irreversible thermodynamics indicates that, for a simple spherical source model, potentials generated by electrokinetic coupling may be of greater amplitude than those developed by thermoelectric coupling. Before any more quantitative interpretations of potentials generated by geothermal activity can be made, analytical solutions for more realistic geometries must be developed, and values of _in situ_ coupling coefficients must be obtained.

If the measuring electrodes are not watered, and if telluric currents and changes in electrode polarization are monitored and corrections made for their effects, most self-potential measurements are reproducible within about ±5 mV. Reproducible short-wavelength geologic noise of as much as ±10 mV, primarily caused by variation in soil properties, is common in arid areas, with lower values in areas of uniform, moist soil. Because self-potential variations may be produced by conductive mineral deposits, stray currents from cultural activity, and changes in geologic or geochemical conditions, self-potential data must be analyzed carefully before a geothermal origin is assigned to observed anomalies.

Self-potential surveys conducted in a variety of geothermal areas show anomalies ranging from about 50 mV to over 2 V in amplitude over

distances of about 100 m to 10 km. The polarity and waveform of the observed anomalies vary, with positive, negative, bipolar, and multipolar anomalies having been reported from different areas. Steep potential gradients often are seen over faults which are thought to act as conduits for thermal fluids. In some areas, anomalies several kilometers wide correlate with regions of known elevated thermal gradient or heat flow.

Introduction

Self-potential anomalies that appear to be related to geothermal activity have been reported from a considerable number of geothermal areas. In this paper we discuss some possible source mechanisms for these anomalies, and give examples of noise and data reproducibility problems that often are encountered in self-potential work, and are more severe in large-scale geothermal surveys than in the relatively small-scale surveys conducted for mineral exploration. We then briefly summarize previously reported self-potential surveys conducted in geothermal areas and present recent results from five additional areas: Grass Valley, Nevada; Cerro Prieto, Baja California, Mexico; Mono Lake, California; Roosevelt Hot Springs, Utah; and Steamboat Springs, Nevada.

Possible mechanisms of self-potential generation by geothermal activity

Although the observed self-potential anomalies described later in this paper appear to be related to geothermal activity, the mechanism by which these anomalies are generated is not well understood at this time. However, there is evidence that both the elevated temperature and the circulation of subsurface fluids which are characteristic of geothermal systems are capable of generating surface potential fields comparable in wavelength and amplitude to the self-potential anomalies observed in geothermal areas. The mechanisms by which elevated temperature and the flow of subsurface fluids may generate such anomalies are discussed below.

1. Thermoelectric Coupling

If a temperature gradient is maintained across a sample of rock, a corresponding voltage gradient will appear across the sample. This phenomenon is known as thermoelectric coupling, and may be caused by differential thermal diffusion of ions in the pore fluid and of electrons and donor ions in the rock matrix; a process known as the Soret effect (Heikes and Ure, 1961). The ratio of the voltage to the temperature difference, $\Delta V/\Delta T$, is called the thermoelectric coupling coefficient.

Data presented by Nourbehect (1963) for a variety of rock types give thermoelectric coupling coefficients ranging from -0.09 to +1.36 mV/$^{\circ}$C, with an average value of about 0.27 mV/$^{\circ}$C. Dorfman _et al_. (1977) obtained coefficients ranging from about 0.3 to 1.5 mV/$^{\circ}$C for a variety of sandstone, limestone and serpentenite samples. In a related experiment by Dorfman _et al_. (1977), a point heat source of 49°C inserted near the center of a limestone block measuring about 2 x 1 x 1 m was seen to immediately generate a surface potential field of about +20 mV amplitude centered over the heat source. In an experiment using powdered and crystalline pyrite samples, Yamashita (1961) measured a coupling coefficient of about -0.25 mV/$^{\circ}$C.

A technique based on the concepts of irreversible thermodyanmics to yield surface self-potential fields generated by subsurface thermoelectric coupling is described by Noubehecht (1963). This approach requires the presence of a boundary that separates regions of differing thermoelectric coupling coefficients and is intersected by a body of elevated temperature relative to its surroundings.

Curves showing the thermoelectric potential generated by a sphere of uniform elevated temperature are given by Nourbehecht (1963). As a first approximation to a geothermal model, we consider a buried sphere centered at a depth equal to its diameter and intersected through its center by a horizontal boundary separating an upper layer of conductivity σ_1 from an infinitely deep lower layer of conductivity 3 σ_1 (Fig. 1). For this case, the maximum surface potential is about 0.15 $[(C_1-C_2)\Delta T]$ mV, where C_1 and C_2 are the thermoelectric coupling coefficients of the upper and lower layers, respectively, and ΔT is the temperature difference between the sphere and its surroundings.

For a large value of (C_1-C_2) of 1 mV/^{o}C and a ΔT of 100^{o}C the maximum potential is about 15 mV, and for a more realistic value of (C_1-C_2) of 0.2 mV/^{o}C the maximum potential is about 3 mV. The polarity of the anomaly depends on the sign of (C_1-C_2). This is an important point, as it indicates that thermoelectric anomalies may be of either positive or negative polarity.

Anomalies generated by this model are of smaller amplitude than usually seen in geothermal areas, and they would be difficult to distinguish from typical background noise (discussed later in this paper). More concentrated areas of high temperature at shallow depth, such as thermal fluids in a fault zone, could result in anomalies of shorter wavelength and greater amplitude, which would be more readily detectable. If the relatively long-wavelength (several km), large-amplitude (50 mV or more) anomalies seen in some geothermal areas are generated by thermoelectric coupling, either the *in situ* thermoelectric coupling coefficients are larger than those measured in the laboratory, or the sources are of different geometry than the sphere model considered above. More quantitative interpretation of possible thermoelectric effects awaits the measurement of *in situ* thermoelectric coupling coefficients in geothermal areas, and the development of analytical methods to calculate the surface self-potential expression for more realistic geothermal models.

Several field examples seem to indicate that measurable self-potentials may be generated by elevated subsurface temperatures. A series of measurements made by Dorfman *et al.* (1977) over steam and fire flood wells used for secondary recovery of petroleum at depths of about 200 m showed positive self-potentials which correlated with the location of the steam or fire front as determined from temperatures at the heads of recovery wells. In this case, the steep gradients of the surface potential field implied that some sort of vertical structure may have influenced the surface expression of the potential field generated at depth. Electrokinetic coupling (discussed later in this paper) also may have contributed to the anomaly. The boundaries of the self-potential anomalies measured at Leach Hot Springs, Nevada (Figs. 6 and 7), Mono Lake, California (Fig. 10), and Roosevelt Hot Springs, Utah (Fig. 11) appear to correlate with the limits of areas of known anomalously high heat flow, allowing the possibility that at least a portion of these anomalies was generated by thermoelectric coupling.

Self-potential surveys conducted over shallow coal burns provide additional examples of possible thermoelectric coupling in the earth. On the assumption that a shallow coal mine fire might be a good model of a miniature geothermal system, surveys were made of two shallow burns. A survey at Marshall, Colorado (Fig. 2) shows a well-defined negative anomaly of 140 mV peak amplitude centered over what appeared to be the burning region as evidenced by smoke and steam issuing from some vents. The coal seam is at a depth of about 10 m and is capped to the surface by sandstone.

A survey of a coal burn at Acme, Wyoming gave similar results. In one area the burn was at most 3 m below the surface and rocks glowing red 30 cm below the surface could be seen in slump cracks. A positive anomaly of about 30 mV maximum amplitude was associated with this extreme thermal gradient. Larger anomalies were noted where the overburden was thicker, possibly indicating that electrokinetic effects were augmenting the thermoelectric component.

2. <u>Electrokinetic coupling</u>

The flow of a fluid through a porous medium may generate an electric potential gradient (called the electrokinetic or streaming potential) along the flow path by the interaction of the moving pore fluid with the Helmholtz double layer at the pore surface, a process known as electrokinetic coupling (MacInnes, 1961). The streaming potential, E, generated by the flow of fluid through a capillary tube is given by

$$E = \frac{\rho \varepsilon \zeta}{4 \pi \eta} \Delta P \,, \tag{1}$$

where ρ, ε, and η are, respectively, the electrical resistivity, dielectric constant, and viscosity of the pore fluid; ΔP is the pressure drop along the flow path (related through Darcy's law to the fluid viscosity and flowrate and permeability of the medium); and ζ, the zeta potential, is the voltage across the Helmholtz double layer. Not enough is presently known about the behavior of ρ, ζ, and η in the pores of rocks and soil to allow direct calculation of the electrokinetic coupling coefficient $E/\Delta P$. As ζ may be either positive or negative (Dakhnov, 1962), E may either increase or decrease along the flow path.

Measured values of the streaming potential coupling coefficient $E/\Delta P$ in a variety of rocks listed by Nourbehecht (1963) range from -12 to +31 mV/atm in sandstones with distilled water used as the pore fluid. Tuman (1963) obtained $E/\Delta P$ values of about 150 to 390 mV/atm using 500 ohm-m distilled water in porous sandstones, and about 15 mV/atm using 4.4 ohm-m water. Ahmad (1964) obtained $E/\Delta P$ values in quartz sands ranging from 50 mV/atm for 24 ohm-m pore fluid to about 2400 mV/atm for 2700 ohm-m pore fluid, and similar results were obtained by Ogilvy et al. (1969). The measurements in quartz sands also revealed that $E/\Delta P$ is affected by the permeability and grain size of the matrix, factors that do not appear explicitly in (1). The flow of steam in pipes has been seen to generate very large potentials (Klinkenberg and van der Minne, 1958) so it is possible that electrokinetic coupling coefficients for subsurface steam flow may be greater than those listed above for fluid flow.

Self-potential fields produced by the flow of subsurface water have been observed by Ogilvy et al. (1969), who measured variations of as much as 50 mV over zones of water leakage through fissures in the rock floor of a reservoir; and by Bogoslovsky and Ogilvy (1973), who obtained a positive anomaly of 55 mV amplitude that mirrored the groundwater depression cone surrounding a well pumping from a depth of 16 m. Streaming potentials are thought to be the most reasonable explanation for the self-potential anomalies described by Zablocki (1976), Combs and Wilt (1976), Zohdy et al. (1973), and Anderson and Johnson (1976). As discussed later in this paper, the self-potential contours at Leach Hot Springs, Nevada strongly resemble the pattern of near-surface water flow. Onodera (1974) observed that the self-potential measured across a stationary dipole near a production well in the Otake field, Japan (the length, location and orientation of the dipole are not specified) varied by 28 mV as the flow of the well was turned off and on, the variation being attributed to streaming potentials.

A technique for calculating self-potential fields generated by electrokinetic coupling is given by Nourbehecht (1963). This technique uses the concepts of irreversible thermodynamics to describe the coupling of pressure and potential gradients, and requires that a component of the pressure gradient be parallel to a boundary separating regions of differing electrokinetic coupling coefficients in order for a surface self-potential field to be developed by subsurface fluid flow.

The only electrokinetic model described explicitly by Nourbehecht is a buried spherical pressure souce (or sink) in a horizontally layered medium. Although a spherical source probably is not representative of the driving force for fluid flow in a geothermal system, it is instructive to compare surface potential fields generated by this model with those obtained from the thermoelectric case discussed earlier. For the same geometry and resistivity distribution used for the thermoelectric case (Fig. 1), the maximum surface potential above the center of the sphere is about 0.6 $[(C_1-C_2)\Delta P]$ mV, where C_1 and C_2 are the electrokinetic coupling coefficients in mV/atm of the upper and lower layers respectively and ΔP is the pressure difference across the boundary of the sphere in atmospheres.

For a reasonable value of $(C_1 - C_2)$ of 10 mV/atm and a pressure difference of 5 atm the maximum potential over the center of the sphere is about 30 mV, about an order of magnitude greater than for the reasonable thermoelectric case discussed previously. The polarity of the anomaly depends on the sign of $(C_1 - C_2)$ and the direction of the pressure gradient, so anomalies may be of either polarity. Thus, for similar geometry, self-potential anomalies generated by electrokinetic coupling might be expected to be larger in amplitude than those generated by thermoelectric coupling.

An important point of this discussion is that the magnitude and polarity of self-potential anomalies generated by thermoelectric and electrokinetic coupling depend not only on source parameters such as temperature, pressure, and geometry, but also on the magnitudes and differences of the coupling coefficients. Thus even if substantial subsurface temperature and pressure gradients exist in an area, a measurable self-potential anomaly will not be generated unless the coupling coefficients and their differences across boundaries are sufficiently large. Also, even though both driving forces (temperature and pressure) may be present, the contribution of each to the total anomaly will depend on the relative magnitude of the coupling coefficients and their differences. These magnitudes may vary not only from one geothermal area to another, but also from point to point within the same area. Therefore, knowledge of in situ coupling coefficients is necessary before any quantitative comparison between thermoelectric and electrokinetic contributions to a given self-potential anomaly may be made.

Noise sources and data quality

Self-potential surveys made for conductive mineral exploration often are plagued by high noise levels and poor data reproducibility, problems which have cast the method into some disrepute. These problems are compounded in geothermal surveys, where the wavelength of the anomalies tends to be much longer, and their amplitude smaller than typical for shallow conductive mineral deposits. The long survey lines needed for profiling in geothermal areas increase errors caused by telluric current variations and electrode drift, and the typical geologic background noise level of ±5 to ±10 mV may interfere with the detection of anomalies of the same magnitude. Survey procedures, such as stepwise advancement of a short measuring dipole ("leapfrog" technique) or the watering of electrodes to improve ground contact, which are adequate for the detection of the short-wavelength, high-amplitude anomalies that are typical of shallow conductive mineral deposits (Sato and Mooney, 1960) have lead to serious cumulative errors when used over long survey lines. As the necessary precautions for obtaining reliable data in large-scale self-potential surveys are not treated in detail in the standard references on the method (e.g., Parasnis, 1966 ; Broughton Edge and Laby, 1931), the sources of noise and error for such surveys are discussed briefly in the following sections.

1. Telluric currents

Long-period telluric currents generated by temporal variations in the earth's magnetic field may be much as several hundred mV/km over resistive terrain (Keller and Frischknecht, 1966). Much of this telluric activity is between 10 and 40 seconds in period, but there is also considerable energy at longer periods. If significant variations of 10 to 40 second periods occur while a self-potential measurement is being made, several successive peaks and troughs may be averaged to give a reasonable approximation to the true "DC" value. Variations with periods greater than about one minute, however, are much more difficult to recognize during a typical measurement period of less than one minute, and may be erroneously assumed to be spatial variations. An estimate of the level of long-period telluric activity may be gained by recording telluric variations across a stationary dipole in the survey area, but quantitative corrections to the data may be made only if the apparent resistivity of the earth beneath both the stationary dipole and the survey point is known for a period equal to that of a recorded variation.

Telluric variations generally are not as serious a problem in relatively conductive valleys as in mountainous areas, where resistivities usually are higher, lateral resistivity variations are more prominent, and the direction of the currents may vary considerably. Even under ideal geologic conditions, self-potential measurements taken during magnetic storms may exhibit very high noise levels.

2. Streaming potentials

As discussed above, electrokinetic coupling may be one of the mechanisms by which geothermal activity generates self-potential anomalies. Such potentials generated by the flow of non-thermal subsurface water would constitute a noise source in geothermal prospecting, and may be a major cause of variations related to topographic effects that are sometimes observed in self-potential data (Williams et al., 1976; Poldini, 1939).

An extreme example of a topographic effect possibly related to streaming potentials was noted in a survey on Adak Island in the Aleutian chain of Alaska, where self-potential measurements were made in conjunction with other electrical studies to assess the geothermal potential around Adagdak volcano. A strong correlation between a self-potential profile and elevation is seen in Figure 3. The topographic peak of Adagdak, at an elevation of 645 m, was 2693 mV negative with respect to a reference at 15 m above sea level. Because of the large amount of rain on Adak, a streaming potential mechanism provides a reasonable explanation for the observed correlation of self-potential with elevation. Adagdak is normally covered with rain clouds above the 300 m elevation, and snow fields were present in August when the work was done, so an abundant supply of water was available. Assuming that a hydrostatic head due to a water table elevation difference is the driving mechanism, an electrokinetic coupling coefficient of about 100 mV/atm is indicated for the upper slope of Adagdak. This is a reasonable value considering that the ground water is low in dissolved solids and therefore has relatively high resistivity. In this area, the topographically related potential completely overshadowed any possible anomaly caused by geothermal activity. The lack of detailed knowledge of the surface hydrology and of in situ electrokinetic coupling coefficients make it difficult to correct quantitatively for this large potential.

3. Conductive mineral deposits

Deposits containing conducting sulfides such as pyrite, phrrhotite, chalcopyrite, chalcocite and covellite, as well as deposits of magnetite, covellite, and graphite are known to generate self-potential anomalies which almost invariably are negative in polarity over the top of the deposit. The anomalies may be as much as 100 mV in amplitude and seldom exceed a few hundred meters in width (Sato and Mooney, 1960). Sato and Mooney (1960) propose a mechanism for these anomlies in which the conductive mineral deposit serves as a path for electrons to travel upward throgh the deposit, from the reducing environment at depth to the oxidizing environment at the upper end of the deposit. The corresponding flow of groundwater ions in the earth surrounding the deposit generates the observed anomaly. As conductive minerals, unrelated to present-day geothermal activity, often occur in geothermal areas, their anomalies could present a noise source in geothermal surveys. An example of such an anomaly in shown in Figure 4. The large scale of the anomaly and its onset coincident with Kyle Hot Springs appeared to be of geothermal interest, but test holes at locations KY-1 and KY-3 showed an extensive zone of conductive graphite (with pyrite in KY-3) beginning at a depth of about 40 m (Goldstein, et al., 1976). As heat flow values in the holes were normal for the area, it seems reasonable to infer that the anomaly was caused by the conductive mineralization, operating through the mechanism described above.

4. Cultural activity

Stray currents generated by cultural activity are a major problem in populated (and some unpopulated) areas. Such currents may be generated by power lines, electrical ground, corrosion of pipelines or buried metallic junk, the action of pipeline corrosion protection systems, well casings, and other geophysical activities in the survey area. The currents may be steady, or may take the form of individual spikes or pulses, series of sinusoidal or square waves, or irregular variations, and may attain amplitudes of tens or hundreds of mV/km at distances greater than 5 km from the source (Hoogervorst, 1975). The use of a telluric monitoring dipole, as mentioned previously, along with careful observations for possible sources of stray currents, is essential to avoid interpreting voltages generated by such currents as natural self-potentials.

5. Resistivity variations and uneven topography

The thermoelectric and electrokinetic processes described previously act essentially as underground current sources. The surface potential fields generated by these sources will be influenced by the subsurface resistivity distribution, and the self-potential field generated by a geothermal source may be distorted by resistivity changes across faults or contacts which are not thermally active. In some cases these self-potential variations may be useful for structural mapping, but care must be taken not to confuse them with anomalies generated by actual thermal activity. As discussed previously, currents produced by telluric activity also are influenced by the resistivity distribution, causing variations in the surface potential field. An example of distortion of a geothermally generated self-potential field caused by a change in resistivity across a contact is seen in the Cerro Prieto data (Fig. 8), discussed later in this paper. Near-surface resistivity variations also may be responsible for some of the large-amplitude, short-wavelength noise often superimposed on longer wavelength self-potential anomalies in the vicinity of a geothermal source.

Uneven topography may affect surface potential fields by distorting current flow patterns (Grant and West, 1965). As near-surface resistivity also may vary considerably from point to point in areas of uneven topography, it may be difficult to separate the topographic and resistivity effects (non-geothermal streaming potentials also may be generated in such areas). A possible example of these combined effects is seen in the eastern portion of the self-potential profile from Roosevelt Hot Springs (Fig. 11), where the noise level increased considerably in an area of extremely uneven topography.

6. Electrochemical effects

Variations in soil chemistry, temperature, or moisture content probably account for much of the background noise seen in self-potential data. The profile along line A-A' in Grass Valley, Nevada (Fig. 6) shows typical background noise of as much as ±10 mV in desert areas. This noise may have wavelengths as short as a few cm, and its amplitude usually is less in areas of moist or more uniform soil. These environmental variations affect the "non-polarizing" electrodes used for field measurements and may result in irreproducible polarization and drift. Preliminary laboratory and field data indicate that different electrode types (e.g., copper-copper sulfate, silver-silver chloride, calomel) may respond differently to changes in soil chemistry, moisture content, and temperature, so it is desirable that the electrode type used for a given survey be specified along with the survey results.

a) Electrochemical concentration cells

The potentials generated by chemical concentration cells may reach several hundred mV (MacInnes, 1961), but these values usually will be seen only across bare metallic electrodes, as the liquid junctions of "non-polarizing" electrodes produce counter potentials and limit the overall cell potential to several tens of mV (Corwin, 1976a). Nourbehecht (1963) estimated that about 20 mV might be the maximum expected value for most geochemical concentration cells. Semenov (1974) reported maximum anomalies of about -30 mV across salt marsh areas, and a survey run across a desert salt flat in Buffalo Valley, Nevada showed no apparent effect of the change in soil chemistry between the salt flat area and the surrounding soil. Positive anomalies of 20 to 40 mV over pegmatite veins, and smaller anomalies over silicified zones, have been attributed to electrochemical effects (Semenov, 1974). As the boundary of the anomaly at Leach Hot Springs, Nevada (Figs. 6 and 7) corresponds to that of a silicified area, it is possible that electrochemical effects contribute to the observed self-potential anomaly.

Alunite may be present in areas of hydrothermal alteration. Very large self-potential anomalies of -1800 mV (Gay, 1967) and -700 mV (Kruger and Lacy, 1949) have been attributed to a concentration cell effect caused by the weathering of alunite to sulfuric acid. The presence of alunite in geothermal areas such as the Dome Fault zone of the Roosevelt Hot Springs KGRA (Parry et al., 1976), then, lends additional uncertainty to the interpretation of self-potential anomalies. The pH difference of about 3.3 between the alunite-bearing and background areas described by Gay (1967) would generate only about 200 mV across a hydrogen ion-reference electrode pair, and preliminary laboratory measurements indicate that pH cells generate even smaller potentials across copper-copper sulfate or other non-polarizing electrode pairs. Thus, it remains unclear whether measured self-potentials exceeding a few hundred mV could be generated by hydrogen-ion concentration cells produced by the weathering of alunite. Self-potential surveys conducted by one of us (DBH) across alunite deposits in the Wah Wah mountains, Utah, and at the Randsburgh, California KGRA showed no significant anomalies, so alunite may be present without accompanying self-potential activity.

Even though most electrochemical potentials may be limited to a few tens of millivolts, they tend to obscure small, long-wavelength anomalies which may be of geothermal interest. Their effect may be minimized by careful selection of electrode sites for uniform soil conditions, by filtering the field data to reduce short-wavelength variations, or possibly by measuring soil chemical properties at each electrode site for future data correction. Improved electrode design, such as the use of a double electrolyte chamber to further chemically isolate the electrode element from the soil, also may help to reduce electrochemical effects.

b) Soil moisture and watering of electrodes

Variations in soil moisture content often give rise to self-potential variations, with the electrode in the wetter soil usually becoming more positive (Poldini, 1939). Similar variations are caused by the common practice of watering electrodes to improve electrical contact with the ground. Potential variations caused by watering of electrodes generally do not adversely affect commutated resistivity readings, but may seriously degrade self-potential data.

Figure 5 shows the effect of watering copper-copper sulfate electrodes. The electrodes were placed in an acid clay soil and allowed to stabilize for about 15 min (during this period the potential changed by 3 mV). Then, about 250 ml of water was poured around one electrode, which caused a jump of 14 mV positive with respect to the unwatered electrode. During the 25 min requried for absorption of the water into the soil, the potential of the watered electrode dropped, possibly because of a streaming potential generated by the flow of the water into the soil. When the absorption was complete, the potential rose to a maximum of 22 mV over a period of about 1 hour. The positive potential associated with the watered electrode has been attributed by one of us (DBH) to electrode contact potentials related to a capillary effect (Kruyt, 1952).

When large diameter (>2 cm) non-polarizing electrodes are used in the field, contact resistances rarely exceed 20 k ohm (1 to 10 ohms is typical) if care is taken to insert the electrodes firmly into small pits that penetrate through the dry surface soil layer (usually no more than 10-20 cm deep, even in desert soils). Inexpensive voltmeters of 10^6 ohm input impedance will not draw appreciable current from the electrodes under these conditions, and there is no need to water the electrodes to reduce contact resistance. When using very small diameter (<5 mm) electrodes, contact resistance seldom exceeds 500 k ohms, and voltmeters having 10^9 ohm input impedance have proven satisfactory.

Electrode watering, therefore, may cause persistant electrode potential changes, and elimination of this practice results in improved consistency and reproducibility of self-potential readings. This is particularly true in "leapfrog" surveys, which are subject to positive cumulative error in the traverse direction, caused by the fresher watering of the leading electrode. Natural variations of soil moisture must be carefully noted in the field, with the realization that they may be the cause of self-potential variations of as much as a few tens of millivolts.

c) Electrode polarization and drift

A spurious potential (polarization) will be measured across an electrode pair if the electrolyte or porous junction of the measuring electrode become contaminated with chemical species not ordinarily present in the electrolyte, or if the electrolyte temperature or porous junction moisture contents differ. Polarization may appear suddenly, for example,after contact of the measuring electrode with a highly concentrated groundwater solution or it may be manifested as drift, as when the porous junction of a base station electrode dries or absorbs groundwater ions over a period of time. Drift may also be observed during the course of a single reading, as the temperature, moisture, and chemical content of the electrode adjust to the values in the soil. Minimizing the amount of time an electrode remains in the ground reduces the chance for contamination. Therefore, readings should be made as quickly as possible, consistent with the level of telluric noise activity. Usually, only a few seconds are needed for the electrode to "settle in", with any drift after this period being a response to environmental conditions. Along with telluric variations and time-varying stray currents, polarization and drift constitute the major source of non-reproducibility in most self-potential measurements.

If the electrolyte temperature of the measuring electrode differs from that of the reference, a potential will appear across the electrode pair. The temperature coefficient for saturated copper-copper sulfate electrodes is about 0.5 mV/^{o}C (Ewing, 1939; Poldini, 1939); for silver-

silver chloride electrodes it is somewhat less than half of this value (Corwin and Conti, 1973). The combined polarization and drift caused by these temperature differences, by electrolyte or porous junction contamination, or by drying of the porous junction may be determined during the survey by periodically measuring the voltage between the working electrodes and a reference electrode maintained in a bath of electrolyte solution. The reference electrode maintains a relatively constant potential if its temperature is held constant. This procedure allows polarization and drift corrections to be made to the data. As these corrections may at times amount to some 20 mV, neglecting them may lead to significant errors. An example of data improvement resulting from this procedure is discussed later in this paper, in the description of survey results from Leach Hot Springs, Nevada.

7. Field procedure

It is apparent that much care must be taken to obtain reproducible and meaningful self-potential data. We have found that potential readings are affected by the quality of the electrode contact with the soil, and that this effect is greater than would be predicted from a simple change in circuit resistance relative to the impedance of the measuring instrument. For example, reseating an electrode to reduce the measured circuit resistance from 20 k ohms to 5 k ohms may change the measured potential by 5 or 10 mV, representing a variation of at least several percent for a typical total reading of less than a few hundred mV. For a voltmeter with 10^6 ohm input impedance, a source resistance change of 15 k ohms would cause the indicated voltage to change by only a few tenths of a percent; an amount considerably less than the observed variation. Therefore, electrode contact resistance should be checked at each station, and an effort made to ensure good ground contact and to keep the circuit resistance as uniform as possible from station to station. As the resistance measurement polarizes the electrodes by driving current through them, it should be made after completing the self-potential reading, for as short a time as possible.

Potentials generated by telluric currents should be monitored to assure that they are not misinterpreted as spatial anomalies. Frequent checks of electrode polarization and drift are essential, especially when a "gradient" or "leapfrog" survey configuration (in which a dipole of fixed length is stepped along the survey line, and successive voltages added to obtain the total field) is used. When many such additions are performed, small errors may accumulate to large values. Running such surveys in a closed loop does not provide an absolute check on possible cumulative error, as the polarization of an electrode pair may change magnitude and polarity from reading to reading. Alternating the leading and following electrodes ("leapfrogging") in this type of survey will help to reduce cumulative error caused by electrode polarization. Polarization errors also will affect data for a "total field" survey (in which a fixed base electrode is used for the entire survey) but, as successive readings are not additive as with the "gradient" method, the error of each reading is limited to the maximum value of the polarization. If field measurements are made carefully and the effects of polarization, drift, tellurics, and stray currents are accounted for, most self-potential measurements (if made at identical locations) are reproducible within about ±5 mV, even if taken many years apart (Parasnis, 1970).

Reproducible data, of course, are not necessarily meaningful in terms of geothermal activity. The possibility that the measurements have been affected by non-thermal subsurface water flow, conductive mineral deposits, stray currents (and other cultural effects such as plowed fields, cultivation, irrigation, or agricultural chemicals), or soil moisture or chemistry variations must be carefully considered. These effects may be minimized by judicious selection of survey lines and electrode sites, and careful observation and recording of soil type and condition, local geology, vegetation, topography, and cultural manifestations.

Previously reported self-potential surveys in geothermal areas

Self-potential anomalies of widely varying amplitude, polarity, and spatial extent have been reported from several geothermal areas. Examples from the United States include positive anomalies of as much as 2300 mV in amplitude and about 1 km in width measured on Kilauea volcano, Hawaii by Zablocki (1976); a negative anomaly of about 200 mV amplitude and about 1 km in width at the northwest edge of the Dunes thermal area, California (Combs and Wilt, 1976); a steep-sided positive anomaly of about 30 mV amplitude and 2 km in width over the Mud Volcano area of Yellowstone National Park, Wyoming (Zohdy et al., 1973); a dipolar anomaly covering about 15 km and of about 900 mV peak-to-peak amplitude over a postulated resurgent dome in Long Valley, California (Anderson and Johnson, 1976); narrow dipolar anomalies of about 60 mV maximum amplitude in areas of known near-surface hot water in the Raft River Valley, Idaho (Williams et al., 1976 ; Mabey et al., this volume); and a negative anomaly of about 60 mV amplitude and 3 km in width centered over the Leach Hot Springs area of Grass Valley, Nevada (Corwin, 1976a) (an updated version of this survey is discussed below).

Examples from outside the United States include positive anomalies a few hundred meters wide and as much as 400 mV amplitude measured in the Manikaràn section of the Parbàti Valley geothermal zone, India (Jangi et al., 1976); potential gradients of more than 10 mV/m over electrode spacings of 20 to 50 m in the Aeolian Islands and near Naples, Italy (Rapolla, 1974); and negative anomalies of about 100 mV amplitude and several hundred meters wide extending along fault lines of previously known geothermal activity in the Otake geothermal field, Kyushu, Japan (Onodera, 1974). This last example is expecially interesting, as similar self-potential indications in an area of the field where geothermal activity had not been previously observed apparently helped locate test wells which proved productive enough to lead to the construction of a power plant.

Results of recent surveys

1. Leach Hot Springs area, Grass Valley, Nevada

The results of a self-potential survey made in August 1974 over the Leach Hot Springs area of Grass Valley, Nevada were described by Corwin (1976a). Data taken along line A-A' are shown in Figure 6, and the location of the line is shown in Figure 7. As the wire reel used for this survey held only 500 m, a new base station was established every kilometer, intermediate readings made every 50 or 100 m to the north and south of the base, and the readings tied to those made from the previous base at the 500 m stations. Polarization and drift of the copper-

copper sulfate electrodes were not monitored, so no corrections to the data were made for these effects.

Self-potential measurements in the same area were repeated in September 1975, using a base electrode located at 4.2 km north on line A-A' and a reel holding 5 km of wire, allowing the base electrode to remain at the same location throughout the entire survey (including all the other survey lines shown in Figure 7). Survey electrode polarization was determined by periodically measuring the potential between the survey electrode and a portable reference electrode carried in a bath of copper sulfate solution. The readings were corrected by subtracting the polarization values from the observed measurements, with correction values linearly interpolated between polarization measurements.

The results of the 1975 survey along line A-A' are shown in Figure 6. Station locations were within a few meters of the 1974 ones, and readings generally were made every 100 m instead of the 50 m interval used for most of the 1974 survey. A change in the nature of the data between the two surveys is apparent, with the potentials for the 1975 data returning to a constant level on either side of a negative anomaly surrounding the hot springs area. Although many of the shorter-wavelength variations (up to 1 or 2 km) are similar for the two surveys, cumulative error in the earlier survey, caused by repeated movement of the base electrode and lack of correction for electrode polarization, resulted in a spurious offset of about 30 mV between the north and south ends of the line, and obscured the true nature of the negative anomaly surrounding the hot springs area.

Self-potential contours for the Leach Hot Springs area, based on the smoothed 1975 data, are shown in Figure 7A. A negative anomaly of about 50 mV amplitude encloses the hot spring area and shows maximum activity close to the surface expression of a fault which is thought to act as a conduit for the thermal water (Olmsted et al., 1975). The boundary of the self-potential anomaly roughly coincides with the 2 HFU contour given by Olmsted et al.(1975), shown in Figure 7B, and with the boundary of a positive P-wave velocity anomaly and an electrically resistive silica zone surrounding the hot spring area (Beyer et al., 1976). Total hot spring flow at Leach Hot Springs is about 12 liters/sec at an average temperature of about 78°C (Olmsted et al., 1975). To date, no deep drilling has been done in the area, so the extent of any additional geothermal activity is not known.

The negative self-potential anomaly just to the north of the hot springs coincides with an area where the heat flow is high and the near-surface groundwater level drops sharply (Fig. 7B). Although not enough information is available to allow the contribution to the self-potential anomaly from these two effects to be separated, the similarity of the water table and self-potential contours in this area suggests an electrokinetic mechanism. The water table drops about 50 m, equivalent to a pressure difference of about 5 atm, in the vicinity of the springs. The resistivity of the spring water is about 12 ohm-m (Olmsted et al., 1975) and the rocks in the hot springs area are highly silicified, so an electrokinetic coupling coefficient of 10 mV/atm might not be unreasonable. Thus a 50 mV potential difference could be generated by the 5 atm pressure drop along the flow path, accounting for the similarity between the self-potential and water table contours in the vicinity of the fault.

2. Cerro Prieto geothermal field, Baja California, Mexico

Cerro Prieto, located in northern Baja California, Mexico, is a major geothermal field, presently producing 75 megawatts of electrical energy. Total fluid flow is about 750 metric tons/hr of steam and 2000 metric tons/hr of separated water (Noble *et al*., 1977). Well-head temperatures range from about 250°C to over 300°C and total dissolved solids (primarily NaCl) of the well water vary from about 9000 to 37,000 ppm (Mañon *et al*., 1977).

A self-potential profile, line B-B', run across the producing area of the field is shown in Figure 8. The location of the survey line, and the straight line onto which the data were projected to reduce geometric distortion, are shown in Figure 9. A striking dipolar anomaly with a peak-to-peak amplitude of about 150 mV is centered over the Cerro Prieto fault which is thought to act as a major conduit for the geothermal fluids (Noble *et al*., 1977).

A geologic profile along line B-B' is shown in the center of Figure 8, and an electrical model made in an attempt to define the source geometry of the self-potential anomaly is shown at the bottom of the figure. The model consists of a vertical sequence of ten horizontal current dipoles, separated by 500 m, in a half-space of 3 ohm-m resistivity. The dipole currents, which were chosen by trial and error to produce a potential field which roughly matches the measured data, increase linearly with depth. The dipoles extend from a depth of 1 km to 3.25 km; the zone of the fault along which thermal fluids are thought to flow into the shale and sandstone formation which comprises the geothermal reservoir. The dipoles are only in the plane of the section, and do not extend along the strike of the fault.

The potential field generated by the model corresponds reasonably well with the actual profile in the vicinity of the fault and near the ends of the line. The positive deviation of the actual profile from the theoretical curve beginning at about 1 km W probably is caused by higher resistivity material to the west of this point (well M-6 is not a producer, and the western boundary of the production zone lies between wells M-9 and M-6). The cause of the deviation centered at about 5 km E is not known, as little geologic information is available in this area.

Obviously, this model does not define the mechanism of generation of the anomaly. However, it does demonstrate that anomalies of very long wavelength may be produced by potentials generated in a relatively narrow fault zone, and that the existence of an extensive volume of elevated temperature or fluid circulation is not required for the generation of long-wavelength self-potential anomalies (although such a volume does exist in this case).

Considerable temperature and flow data, along with a number of reservoir core samples, are available for this field. We intend in the near future to measure the thermoelectric and electrokinetic coupling coefficients of the cores, and then to attempt to quantitatively model the potential generating mechanism using a technique presently being developed by D.V. Fitterman of the U.S. Geological Survey (personal communication, 1978). This technique, based on the approach of Nourbehecht (1963), allows the calculation of surface potential fields developed by temperature or pressure gradients in the vicinity of a vertical contact.

3. Paoha Island, Mono Lake, California

In 1976, an offshore self-potential survey was conducted in Mono

Lake, California, near a hot spring area on Paoha Island (Waring, 1965). The measurements were made between silver-silver chloride electrodes separated by 35 m, towed along the water surface behind a small boat (the equipment and procedures used are described by Corwin, 1976b). The survey line, shown in Figure 10, was about 15 m offshore, in water about 15 m deep.

A gradient anomaly with a maximum amplitude of 0.7 mV/35m and a length of 1200 m was measured directly offshore of the hot springs area (Fig. 10). Integration of this gradient anomaly gave a total field anomaly of about 2 mV maximum amplitude peak-to-peak. While the anomaly amplitude is small, it is well above the background noise level of about 0.05 mV/35m. The small amplitude of the anomaly is not surprising in view of the 0.1 ohm-m resistivity of the highly saline lake water.

Thermal gradient measurements made on the lake bottom indicate that the thermal activity continues offshore of the hot spring area on Paoha Island (Welday, 1977). A significant feature of this survey is that the anomaly was measured in homogeneous lake water, precluding possible electrode effects caused by varying soil chemistry, temperature, and moisture content (discussed previously) often encountered in an onshore survey.

4. Roosevelt Hot Springs KGRA, Utah

The Roosevelt Hot Springs KGRA, located near Milford, Utah, is a water dominated geothermal system with maximum temperatures in excess of 265°C (Lenzer et al., 1977). Several production wells have been drilled in the area, and two of these wells are reported to be capable of producing a total mass flow of at least 450 metric tons/hr. The reservoir consists of fractures within crystalline rock, and the depth to the top of the reservoir ranges from about 100 m to more than 1 km. The water contains about 6000 to 8000 ppm of dissolved solids, mainly NaCl. The Dome Fault, which strikes NNE through the area, appears to significantly influence the hydrology, and coincides with the axis of a thermal gradient anomaly (Lenzer et al., 1977; Sill and Bodell, 1977).

A self-potential profile run in early 1977 across the Dome Fault zone is shown in Figure 11. Also shown in the figure are thermal gradient data obtained by Sill and Bodell (1977) along a line roughly coincident with the self-potential line. A broad dipolar self-potential anomaly, extending from about 2.5 km west to about 1 km east, is roughly centered over the Dome Fault. The broad anomaly is interrupted by a steep potential gradient centered directly over the surface trace of the Dome Fault. Some smaller self-potential variations correlate with faults or fault zones (indicated by arrows in Fig. 11) described by Ward and Sill (1976). The large-amplitude, short-wavelength self-potential activity to the east of 1 km east coincides with an area of steep topography and numerous outcrops of granitic rock. As discussed previously, high noise levels might be expected in such areas.

The correspondence between the broad self-potential and thermal gradient profiles suggests a geothermal origin for the self-potential. However, alunite (Ward and Sill, 1976) and pyrite (Parry et al., 1976) are known to be present in the Dome Fault zone. As discussed previously, self-potential activity may be associated with these minerals. The dipolar nature of this anomaly, however, is not typical of self-potential activity related to pyrite or alunite mineralization, which usually is of negative polarity (Sato and Mooney, 1960; Gay, 1967). The shape of the dipolar anomaly is similar to that seen at Cerro Prieto (discussed earlier), and its coincidence with a major fault suggests a similar source geometry; electrical activity with a finite vertical extent concentrated in the fault zone. The short-wavelength dipolar anomaly superimposed on the longer wavelength variation and located directly over the surface trace of the fault could be caused by a separate, shallower zone of geothermally generated electrical activity along the fault.

5. Steamboat Springs, Nevada

Reconnaissance electrical surveys, including self-potential measurements, were made by the U.S. Geological Survey in the Steamboat Springs area of Nevada in 1975 (Fig. 12). The surveys covered the Steamboat Hills, an area of about 21 km^2 west of Highway 395. Detailed self-potential studies were previously made in the eastern part of this area by White et al. (1964). The earlier survey reported considerable difficulty with "fluctuating conditions", which were attributed to "differences in chemical activity, weather, and soil moisture interacting with the porous pot (copper-copper sulfate) electrodes that were used." Station spacing was 50 ft (15.2 m) and positive and negative anomalies of several hundred mV amplitude and as much as 200 ft (61 m) in width were observed, "with no recognized geologic differences to distinguish positive from negative."

Examination of this earlier data shows that areas of opaline and chalcedonic sinter outcrop coincide with large-amplitude (about 100 mV) short-wavelength potential variations, in contrast to other areas where short-wavelength variations were of much smaller amplitude. It appears that extreme electrode polarization effects were responsible for the noise, which tended to obscure other anomalies. White et al. (1964) state that no broad scale trends were found; however, one of their traverses (no. 8) crossed the north end of the principal anomaly found in the 1975 survey. Smoothing of their data shows a dipolar anomaly of 100 mV amplitude and 1200 m width, bounded by negative skirts, which corresponds well with the 1975 data.

In the 1975 reconnaissance survey, a station spacing of 300 m and a leapfrog method of traversing were used in order to cover the large area. As this technique is subject to cumulative errors, three sets of electrodes (one of copper-copper sulfate and two of silver-silver chloride) were used to check electrode polarization. Almost all of the lines were closed, and closure error did not exceed 13 mV with the silver-silver chloride electrodes. The copper-copper sulfate electrodes proved unsatisfactory for this survey because of large drifts, probably caused by polarization effects.

The self-potential contour map (Fig. 12) shows a north-trending positive zone flanked by negative skirts, suggesting a dipolar source, situated between the mud volcano basin and the high terrace. This area is about 1 km west of and 30 m higher in elevation than the Steamboat Springs fault zone, along which the present hot spring activity is concentrated. It is interesting to note that no major long-wavelength anomalies are associated with the Steamboat Springs fault zone although the northern part along the main hot spring terrace is positive with respect to the background. Fault patterns in the Steamboat Hills are rather complex. The faults trend predominantly northeast, northwest, and north, with north trending faults being the most numerous and youngest (White et al., 1964). The negative skirts of the self-potential anomaly are associated with westerly dipping, north trending faults on the northern edge only.

Audio-magnetotelluric surveys and two telluric traverses (Fig. 12) were made in conjunction with the self-potential survey. These data sets all show a low-resistivity trough running north-south along the western edge of the self-potential anomaly and decreasing to the south, about where the self-potential anomaly ends.

Conclusions

Both thermoelectric and electrokinetic coupling mechanisms may generate self-potential anomalies comparable to those observed in geothermal areas. If the local resistivity distribution is known, source geometry may be estimated using standard potential field techniques. Estimates of additional parameters such as the pressure and temperature distribution of the source may be made using an approach described by Nourbehecht (1963). When this approach is applied to a simple spherical source, electrokinetic coupling is seen to generate larger anomalies than thermoelectric coupling for reasonable values of the temperature, pressure, and coupling coefficients. Potentials generated by this model for both thermoelectric and electrokinetic coupling are smaller in amplitude than many observed self-potential anomalies in geothermal areas, implying that the model geometry or the laboratory-measured coupling coefficients are not realistic for geothermal sources. An important point of this analysis is that the size and polarity of self-potential anomalies generated by geothermal activity depend not only on source parameters such as temperature, pressure, and geometry, but also on the magnitude and differences of the coupling coefficients.

Most self-potential measurements are reproducible within about ±5 mV if proper field procedure and data reduction techniques are used. A better understanding of sources of geologic noise and electrode effects could lead to techniques for their removal from field data, allowing more reliable detection of anomalies of amplitude less than a few tens of millivolts. The possibility that observed anomalies may be related to non-geothermal sources, both geologic and cultural, must be considered. As with any other geophysical technique, all other available geological and geophysical information must be used when considering the significance of self-potential data.

Self-potential anomalies ranging in amplitude from about 50 mV to over 2V have been recorded in at least thirteen different geothermal areas around the world. Anomaly shapes show no consistent pattern, although the steepest gradients often are associated with faults thought to be conduits for thermal water, and broad-scale anomalies sometimes roughly coincide with areas of elevated heat flow. The short-wavelength, large amplitude anomalies that often appear to be related to faults in geothermal areas may be produced by relatively shallow thermal fluids in the fault zones,acting through an electrokinetic or thermoelectric coupling mechanism. Also, long-wavelength fields generated by deeper sources may exhibit locally steep gradients over near-surface lateral resistivity boundaries such as faults or contacts.

At this time the most promising uses of the self-potential method in geothermal exploration appear to be for the detection and tracing of faults which control the flow of thermal fluids (often characterized by a dipolar anomaly centered over the fault or by a steep self-potential gradient), and as a reconnaissance technique in searching for areas of elevated heat flow, which may be roughly outlined by broad, relatively smooth self-potential anomalies interrupted by the steep gradients characteristic of fault zones or contacts.

Acknowledgments

This work was supported in part by the U.S. Department of Energy under Contract no. W-7405-ENG-48 to the Lawrence Berkeley Laboratory, University of California, Berkeley, and in part by the U.S. Geological Survey. We thank D.V. Fitterman, C.J. Zablocki, D.R. Mabey, H.F. Morrison, and M.H. Dorfman for their help and criticism. A.L. Lange of AMAX Exploration, Inc. kindly allowed us to use the Roosevelt Hot Springs data, and P. Wilde provided helpful support for the Mono Lake survey.

REFERENCES

Ahmad, M.U., 1964, A laboratory study of streaming potentials: Geophys. Prosp., v. 12, no. 1, p. 49-64.

Anderson, L.A., and Johnson, G.R., 1976, Application of the self-potential method to geothermal exploration in Long Valley, Califnornia, Jour. Geophys. Res., v. 81, no. 8, p. 1527-1532.

Beyer, H., Dey, A., Liaw, A., Majer, E., McEvilly, T.V., Morrison, H.F., and Wollenberg, H., 1976, Preliminary open file report, geological studies in Grass Valley, Nevada: Lawrence Berkeley Laboratory report LBL-5262, Berkeley, California.

Bogoslovsky, V.V., and Ogilvy, A.A., 1973, Deformations of natural electric fields near drainage structures: Geophys. Prosp., v. 21, no. 4, p. 716-723.

Broughton Edge, A.B.,and Laby, T.H., 1931, The principles and practice of geophysical prospecting: Cambridge Univ. Press, London.

Combs, J., and Wilt, M., 1976, Telluric mapping, telluric profiling, and self-potential surveys of the Dunes geothermal anomaly, Imperial Valley, California: Proceedings, Second United Nations Symposium on the Development and Use of Geothermal Resources, San Francisco, Calif., U.S. Government Printing Office, Washington, D.C., v. 2, p. 917-928.

Corwin, R.F., and Conti, U., 1973, A rugged silver-silver chloride electrode for field use: Rev. Sci. Instrum., v. 44, no. 6, p. 708-711.

Corwin, R.F., 1976a, Self-potential exploration for geothermal reservoirs: Proceedings, Second United Nations Symposium on the Development and Use of Geothermal Resources, San Francisco, Calif., U.S. Government Printing Office, Washington, D.C., v. 2, p. 937-945.

Corwin, R.F., 1976b, Offshore use of the self-potential method: Geophys. Prosp., v. 24, no. 1, p. 79-90.

Dakhnov, V.N., 1962, Geophysical well logging: Colorado School of Mines Quarterly, v. 57, no. 2.

Dorfman, M.H., Oskay, M.M., and Gaddis, M.P., 1977, Self-potential profiling--a new technique for determination of heat movement in a thermal oil recovery flood: Preprint, paper presented at 52nd annual meeting, Society of Petroleum Engineers of AIME, Denver.

Ewing, S., 1939, The copper-copper sulfate half-cell for measuring potentials in the earth: American Gas Association Proc. 624.

Gay, S.P., Jr., 1967, A 1800 millivolt self-potential anomaly near Hualgayoc, Peru: Geophys. Prosp., v. 15, no. 2, p. 236-245.

Goldstein, N.E., Beyer, H., Corwin, R., diSomma, D.E., Majer E., McEvilly, T.V., Morrison, H.F., Wollenberg, H.A., and Grannell, R., 1976, Open file report geoscience studies in Buena Vista Valley, Nevada: Lawrence Berkeley Laboratory report LBL-5913, Berkeley, Calif.

Grant, F.S., and West, G.F., 1965, Interpretation theory in applied geophysics: McGraw-Hill, New York.

Heikes, R.R., and Ure, R.W., 1961, Thermoelectricity: Science and Engineering: Interscience, New York.

Hoogervorst, G.H.T.C., 1975, Fundamental noise affecting signal-to-noise ratio of resistivity surveys: Geophys. Prosp., v. 23, no. 2, p. 380-390.

Jangi, B.L., Prakash, G., Dua, K.J.S., Thussu, J.L., Dimri, D.B., and Pathak, C.S., 1976, Geothermal exploration of the Parbati Valley geothermal field Kulu District, Himachal Pradesh, India: Proceedings, Second United Nations Symposium on the Development and Use of Geothermal Resources, San Francisco, Calif., U.S. Government Printing Office, Washington, D.C., v. 2, p. 1085-1094.

Keller, G.V., and Frischknecht, F.C., 1966, Electrical methods in geophysical prospecting: Pergamon, New York.

Klinkenberg, A., and van der Minne, J.L., 1958, Electrostatics in the petroleum industry: Elsevier, New York.

Kruger, F.C., and Lacy, W.C., 1949, Geological explanation of geophysical anomalies near Cerro de Pasco, Peru: Econ. Geol., v. 44, no. 6, p. 485-491.

Kruyt, H.R., 1952, Colloid science: Elsevier, New York.

Lenzer, R.C., Crosby, G.W., and Berge, C.W., 1977, Recent developments at the Roosevelt Hot Springs KGRA: Proceedings, Amer. Nuclear Soc. topical meeting on energy and mineral resource recovery, April 1977, Colo. School of Mines, Golden, Colorado, p. 60-67.

Mabey, D.R., Hoover, D.B., O'Donnell, J.E., and Wilson, C.W., (   ), Reconnaissance geophysical studies of the geothermal system in the southern Raft River Valley, Idaho (this volume).

MacInnes, D.A., 1961, The principles of electrochemistry: Dover, New York.

Mañon, A., Mazor, E., Jiminez, M., Sanchez, A., Fausto, J., and Zenizo, C., 1977, Extensive geochemical studies in the geothermal field of Cerro Prieto, Mexico: Lawrence Berkeley Laboratory Report LBL-7019.

Noble, J.E., Mañon, A., Lippmann, M.J., and Witherspoon, P.A., 1977, A study of the structural control of fluid flow within the Cerro

Prieto geothermal field, Baja California, Mexico: Preprint, 52nd Annual Meeting of the Society of Petroleum Engineers, AIME.

Nourbehecht, B., 1963, Irreversible thermodynamic effects in inhomogeneous media and their application in certain geoelectric problems: Ph.D. thesis, Mass. Inst. of Tech., Cambridge.

Ogilvy, A.A., Ayed, M.A., and Bogoslovsky, V.A., 1969, Geophysical studies of water leakages from reservoirs: Geophys. Prosp., v. 22, no.1, p. 36-62.

Olmsted, F.H., Glancy, P.A., Harrill, J.R., Rush, F.E., and Van Denburgh, A.S., 1975, Preliminary hydrogeological appraisal of selected hydrothermal systems in northern and central Nevada: U.S. Geol. Survey Open File Report 75-76.

Onodera, S., 1974, Geo-electric indications at the Otake geothermal field in the western part of the Kujyu Volcano group, Kyushu, Japan: in Colp, J.L., and Furumoto, A.S., eds., Proceedings of a Conference, The Utilization of Volcano Energy: Sandia Laboratories, Albuquerque, N.M., p. 80-106.

Parasnis, D.S., 1966, Mining geophysics: Elsevier, New York.

Parasnis, D.S., 1970, Some recent geoelectric measurements in the Swedish sulfide ore fields illustrating scope and limitations of the methods concerned: Mining and Groundwater Geophysics, 1967, Geological Survey of Canada, Ottawa, Econ. Geol. Report No. 26, p. 290-301.

Parry, W.T., Benson, N.L., and Miller, C.D., 1976, Geochemistry and hydrothermal alteration at selected Utah hot springs: Nat'l. Science Foundation Final Report, Contract GI43741, Univ. of Utah, Salt Lake City.

Poldini, E., 1939, Geophysical exploration by spontaneous polarization methods: The Mining Magazine, v. 60, p. 22-27.

Rapolla, A., 1974, Natural electric field survey in three southern Italy geothermal areas: Geothermics, v. 3, no. 3, p. 118-121.

Sato, M., and Mooney, H.M., 1960, The electrochemical mechanism of sulfide self-potentials: Geophysics, v. 25, no. 1, p. 226-249.

Semenov, A.S., 1974, Electrical prospecting with the method of the natural electric field: Nedra, Leningrad.

Sill, W.R. and Bodell, J., 1977, Thermal gradients and heat flow at Roosevelt Hot Springs: ERDA Technical Report, Vo. 77-3, Contract EY-76-S-07-1601, Univ. of Utah, Salt Lake City.

Tuman, V.S., 1963, Thermo-telluric currents generated by an underground explosion and other geological phenomena: Geophysics, v. 28, no. 1, p. 91-98.

Ward, S.H., and Sill, W.R., 1976, Dipole-dipole resistivity surveys, Roosevelt Hot Springs KGRA; Final Report, v. 2, to Nat'l Science Foundation, Contract GI-43741, Univ. of Utah, Salt Lake City.

Waring, G.A., 1965, Thermal springs of the United States and other countries of the world: A summary. Revised by R.R. Blankenship and R. Bentall: U.S. Geological Survey Prof. Paper 492, U.S. Gov't. Printing Office, Washington, D.C.

Welday, E.E., 1977, Thermal probe study of Mono Lake, California: <u>in</u> Geothermal investigations of California submerged lands and spherical flow in naturally fractured reservoirs: State Lands Commision, State of California, part D.

White, D.E., Thompson, G.A., and Sandberg, C.H., 1964, Rocks, structure and geologic history of Steamboat Springs thermal area, Washoe County, Nevada: U.S. Geological Survey Prof. paper 458-B, U.S. Gov't. Printing Office, Washington, D.C.

Williams, P.L., Mabey, D.R., Zohdy, A.A.R., Ackerman, H., Hoover, D.B., Pierce, K.L., and Oriel, S.S., 1976, Geology and geophysics of the southern Raft River Valley geothermal areas, Idaho, U.S.A.: Proceedings, Second United Nations Symposium on the Development and Use of Geothermal Resources, San Francisoco, Calif., U.S. Government Printing Office, Washinton, D.C., v. 2, p. 1273-1282.

Yamashita, S., 1961, The electromotive force generated within the ore body by the temperature difference: J. Min. Coll; Akita Univ. (Japan), Ser. A., vol. 1, no. 1, p. 69-78.

Zablocki, C.J., 1976, Mapping thermal anomalies on an active volcano by the self-potential method, Kilauea, Hawaii: Proceedings, Second United Nations Symposium on the Development and Use of Geothermal Resources, San Francisco, Calif., U.S. Government Printing Office, Washington, D.C., v. 2, p. 1299-1309.

Zohdy, A.A.R., Anderson, L.A., and Muffler, L.J.P., 1973, Resistivity, self-potential and induced polarization surveys of a vapor-dominated geothermal system: Geophysics, v. 38, no. 6, p. 1130-1144.

FIGURES

Figure 1 (XBL 787-9595)	Spherical model for thermoelectric or electrokinetic potential generation (after Nourbehecht, 1963). The boundary at depth d separates layers of different resistivity σ and coupling coefficient C. The sphere is at a temperature $100^{o}C$ above the ambient temperature T_o, or at a pressure 5 atm above the ambient pressure P_o. The polarity of the self-potential anomaly depends on the sign of the coupling coefficient difference (C_1-C_2).
Figure 2 (XBL 787-9597)	Self-potential distribution over a coal-mine fire, Marshall, Colorado. Contour interval is 20 mV. Open circles are survey stations.
Figure 3 (XBL 787-9594)	Self-potential vs. ground elevation, Adagdak Volcano, Adak Island, Alaska.
Figure 4 (XBL 787-9592)	Self-potential profile, line B-B', Kyle Hot Springs area, Buena Vista Valley, Nevada. KY-1 and KY-3 are drill-hole locations.
Figure 5 (XBL 787-9598)	Variations in electrode potential caused by watering of copper-copper sulfate electrodes, Raft River, Idaho. Electrode separation was 200 m.
Figure 6 (XBL 787-9596)	Self-potential profiles, line A-A', Leach Hot Springs area, Grass Valley, Nevada. Location of line A-A' is shown in Figure 7A. Upper profile was run in August 1974 and lower profile in September 1975, using improved field techniques described in text. Note typical desert soil background noise level of ±5 to ±10 mV toward north and south ends of 1975 profile.
Figure 7 (XBL 787-9599A)	A. Self-potential distribution in Leach Hot Springs area, Grass Valley, Nevada, based on smoothed data taken in September 1975. SP-A through SP-E, A-A', and E-E' are traverse lines along which measurements were made. Electrode spacing usually was 100 m; contour interval is 10 mV. Faults dashed where inferred. B. Heat flow contours (dashed) and altitude of water table above sea level (solid lines) in the Leach Hot Springs area. (After Olmsted _et al._, 1975).

Figure 8 (XBL 787-9600A)	Self-potential profile (December 1977 and March 1978), geologic cross-section (from Mañon et al., 1977), and electrical model for line B-B', Cerro Prieto geothermal field, Baja California, Mexico. The dashed line on the self-potential profile was generated by the model shown at the bottom of the figure. The location of line B-B' and the straight line onto which the data were projected are shown in Figure 9.
Figure 9 (XBL 787-9593)	Line B-B', Cerro Prieto geothermal field, Baja California, Mexico. That data shown in Figure 8 were projected onto the straight dashed line connecting points B and B' to reduce geometric distortion. The indicated geothermal wells roughly outline the present production zone (the western boundary of the zone is between wells M-6 and M-9). The exact location and strike of the fault which passes between wells M-10 and M-53 are not yet established.
Figure 10 (XBL 787-9601)	Gradient and total field self-potential anomaly in Mono Lake, California, near hot springs area on Paoha Island. Electrodes were towed along the water surface, and water depth was about 15 m.
Figure 11 (XBL 787-9602)	Thermal gradient and self-potential profiles across the Dome Fault, Roosevelt Hot Springs KGRA, Utah. The 0-km point is at the intersection of sections 9, 10, 16, and 15, and the line runs due east-west. Thermal gradient data are from Sill and Bodell (1977). Arrows denote points at which faults mapped by Ward and Sill (1976) cross the self-potential survey line.
Figure 12 (XBL 787-9603)	Self-potential distribution and relative telluric-voltage profiles in the Steamboat Hills area, Nevada. Open circles denote self-potential survey points; closed circles are stations on telluric traverses. Contour interval is 20 mV.

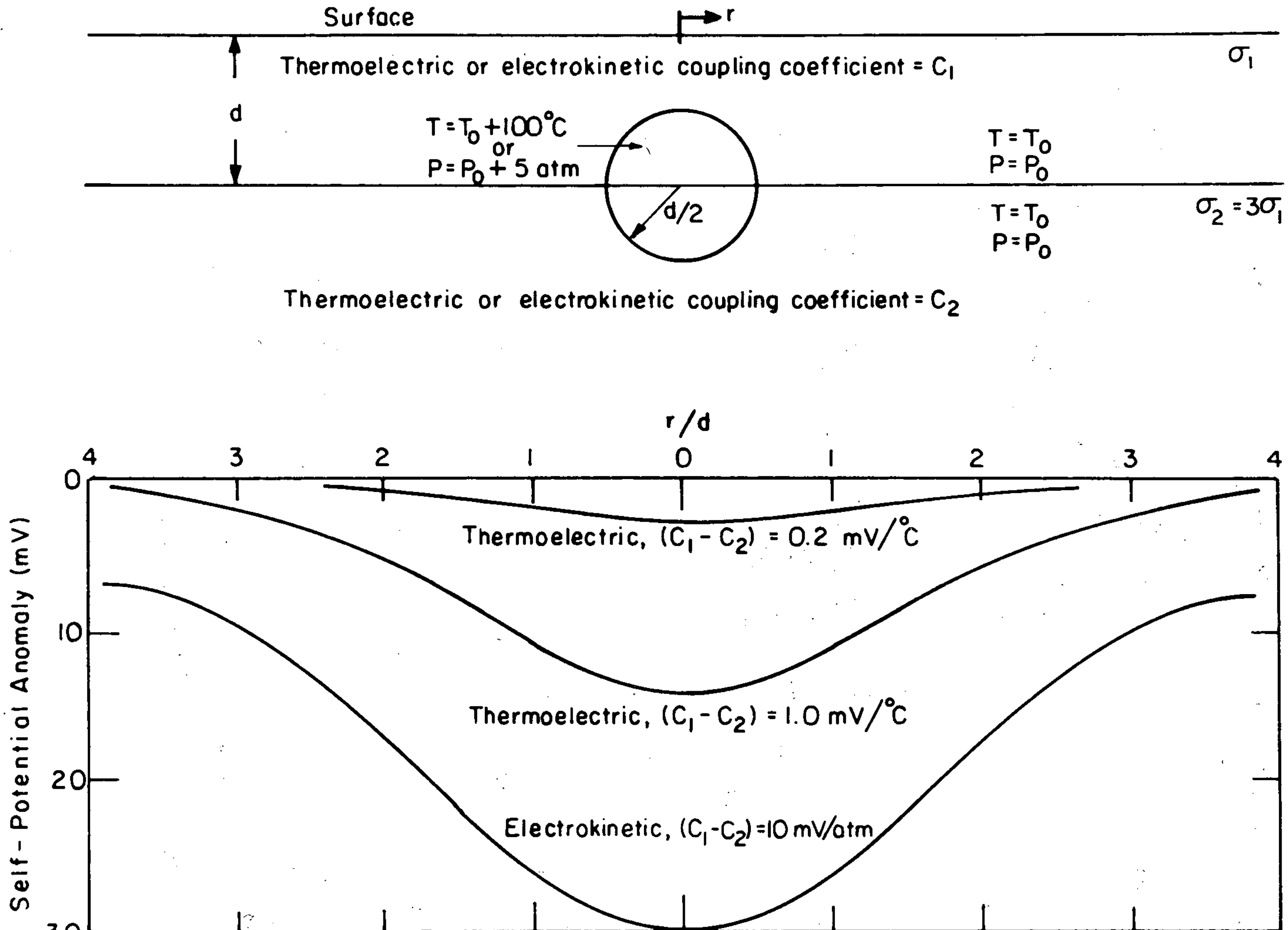

Figure 1

XBL 787-9595

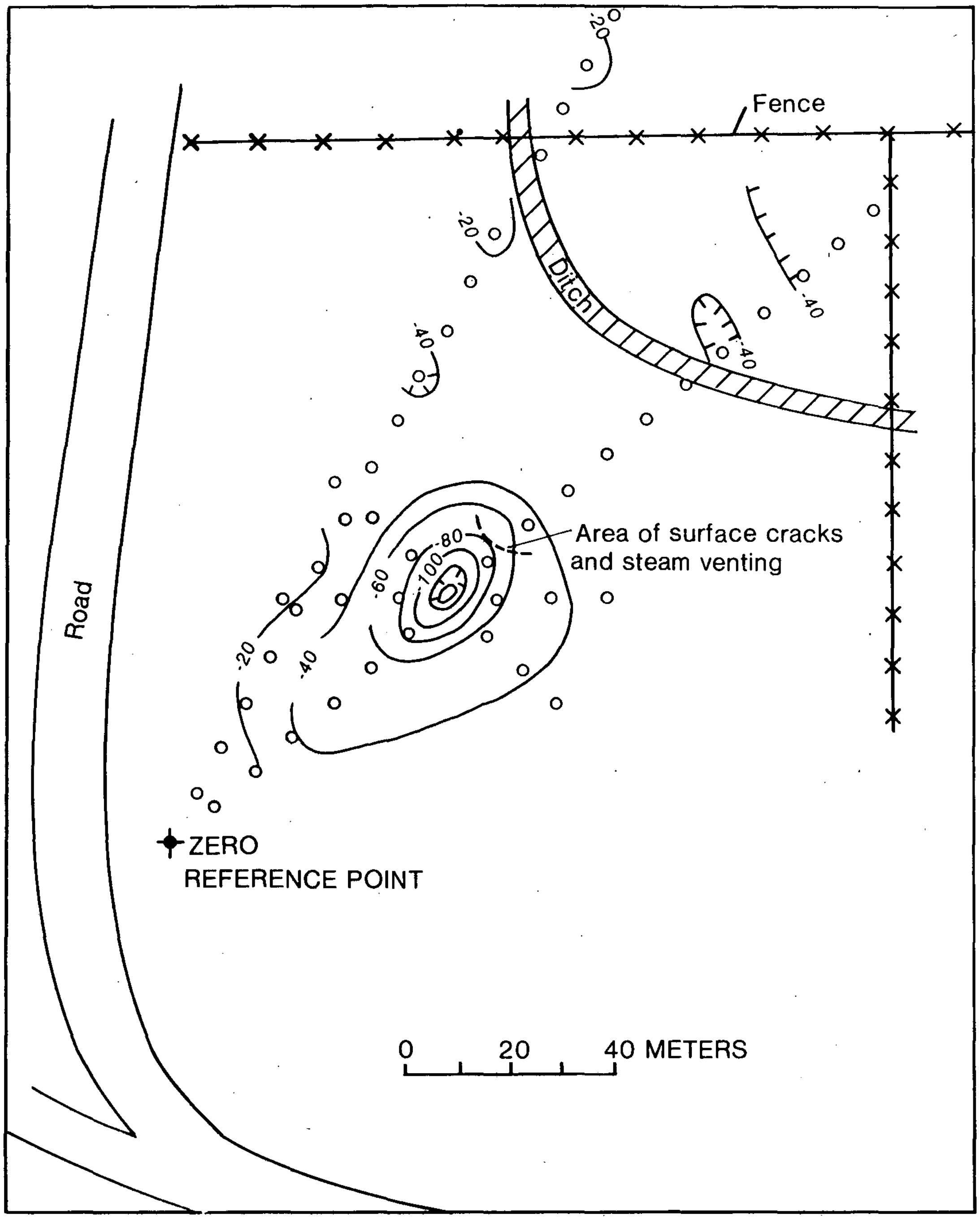

Figure 2

XBL 787-9597

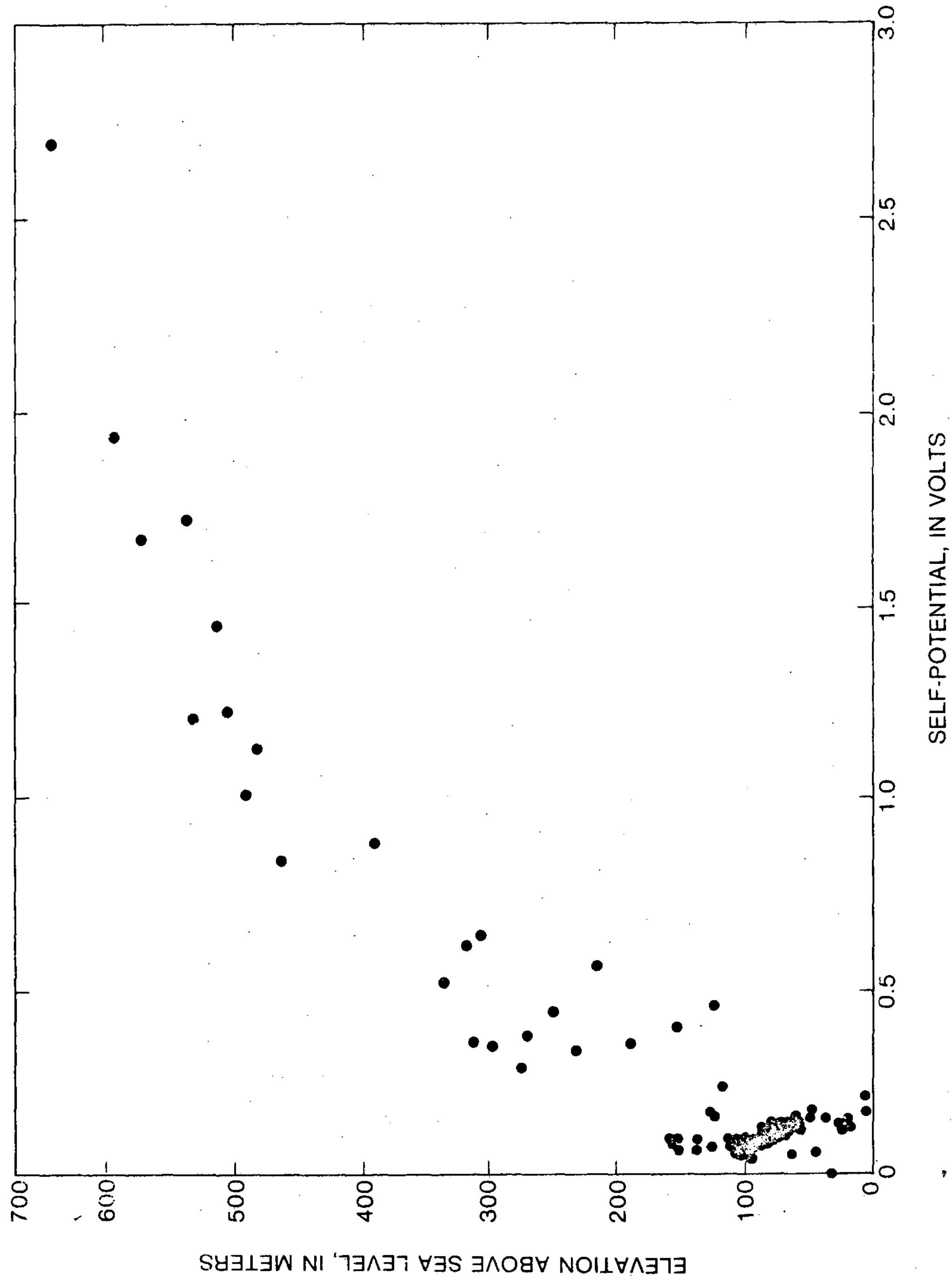

XBL 787-9594

Figure 3

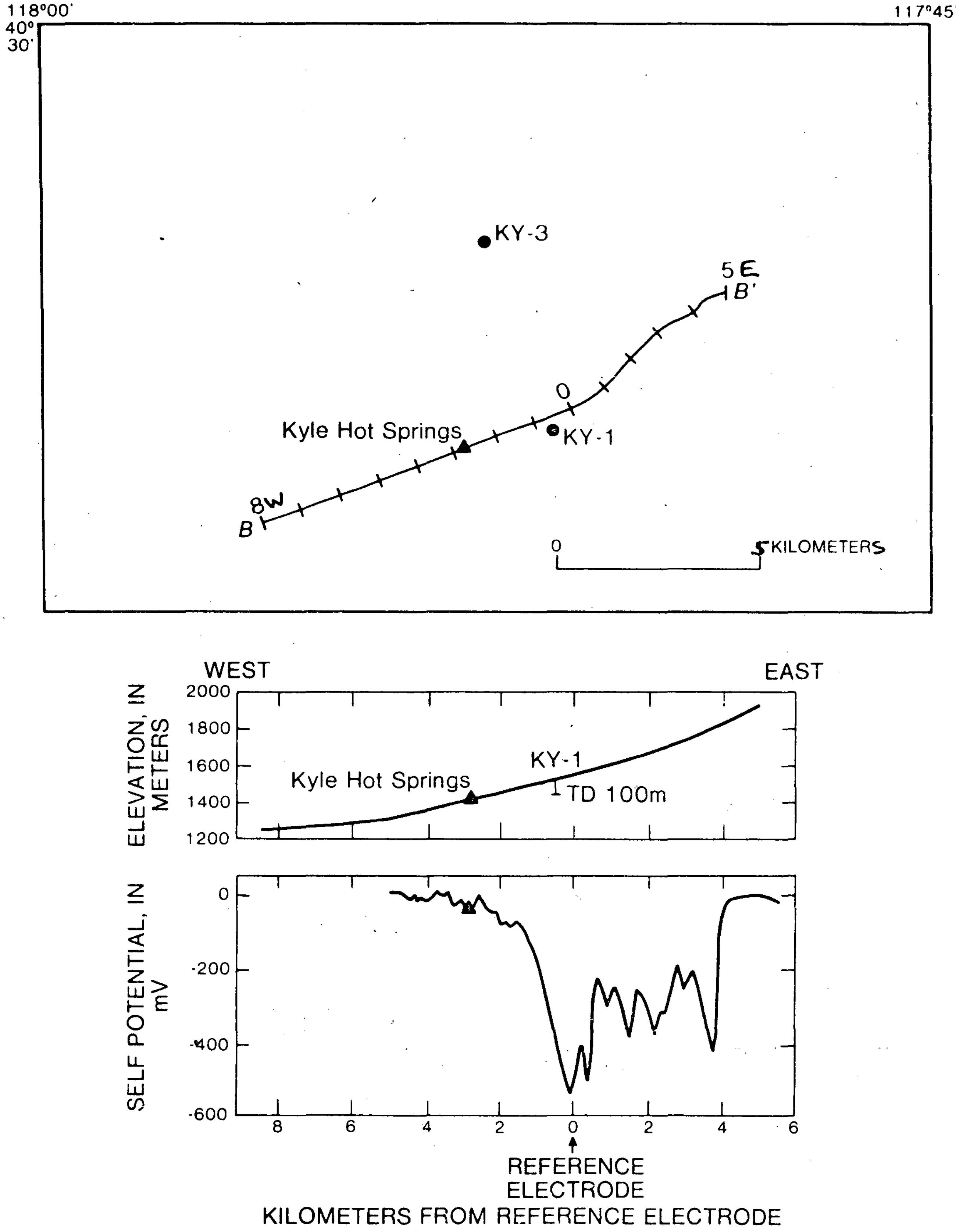

Figure 4

XBL 787-9592

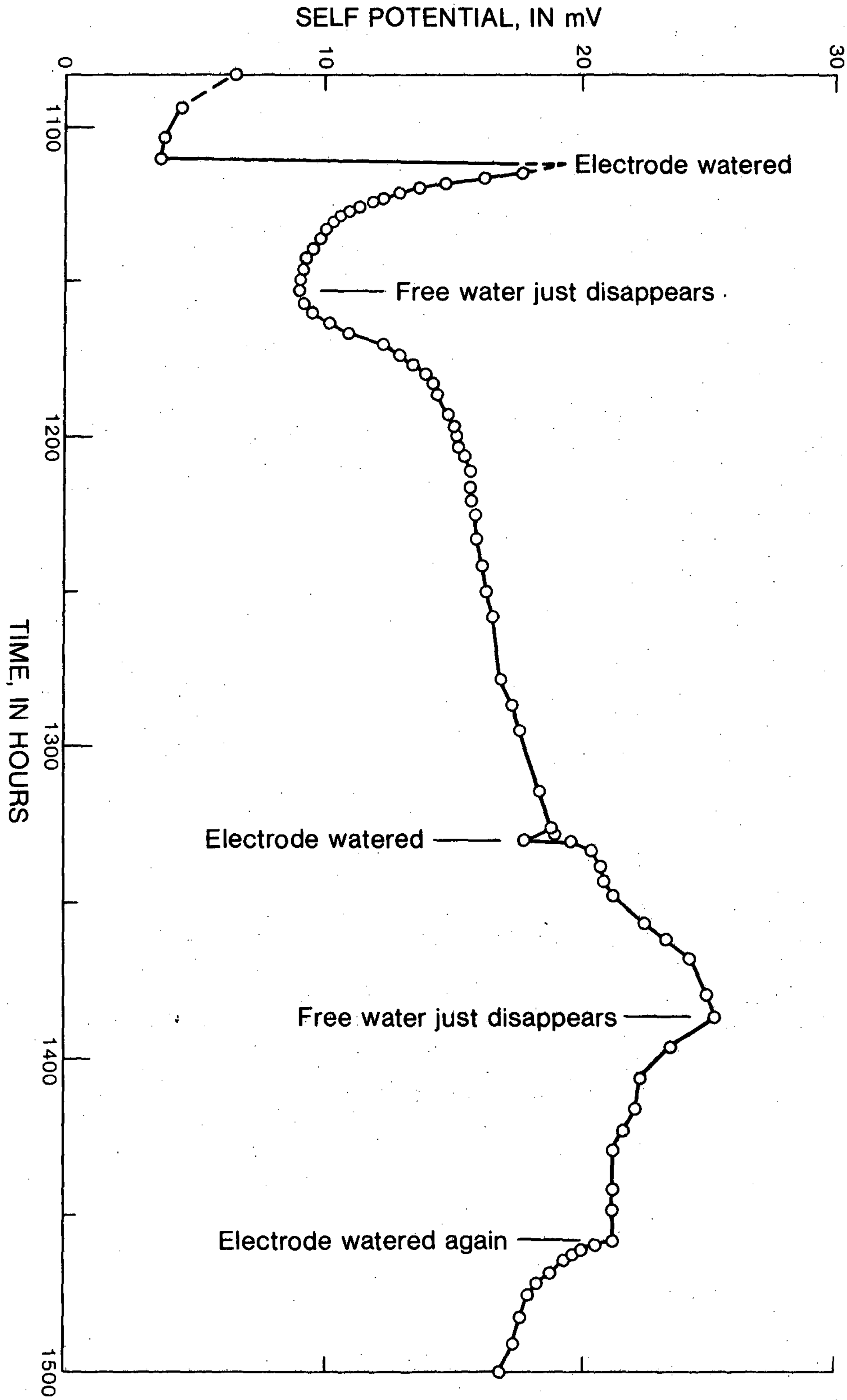

Figure 5

XBL 787-9598

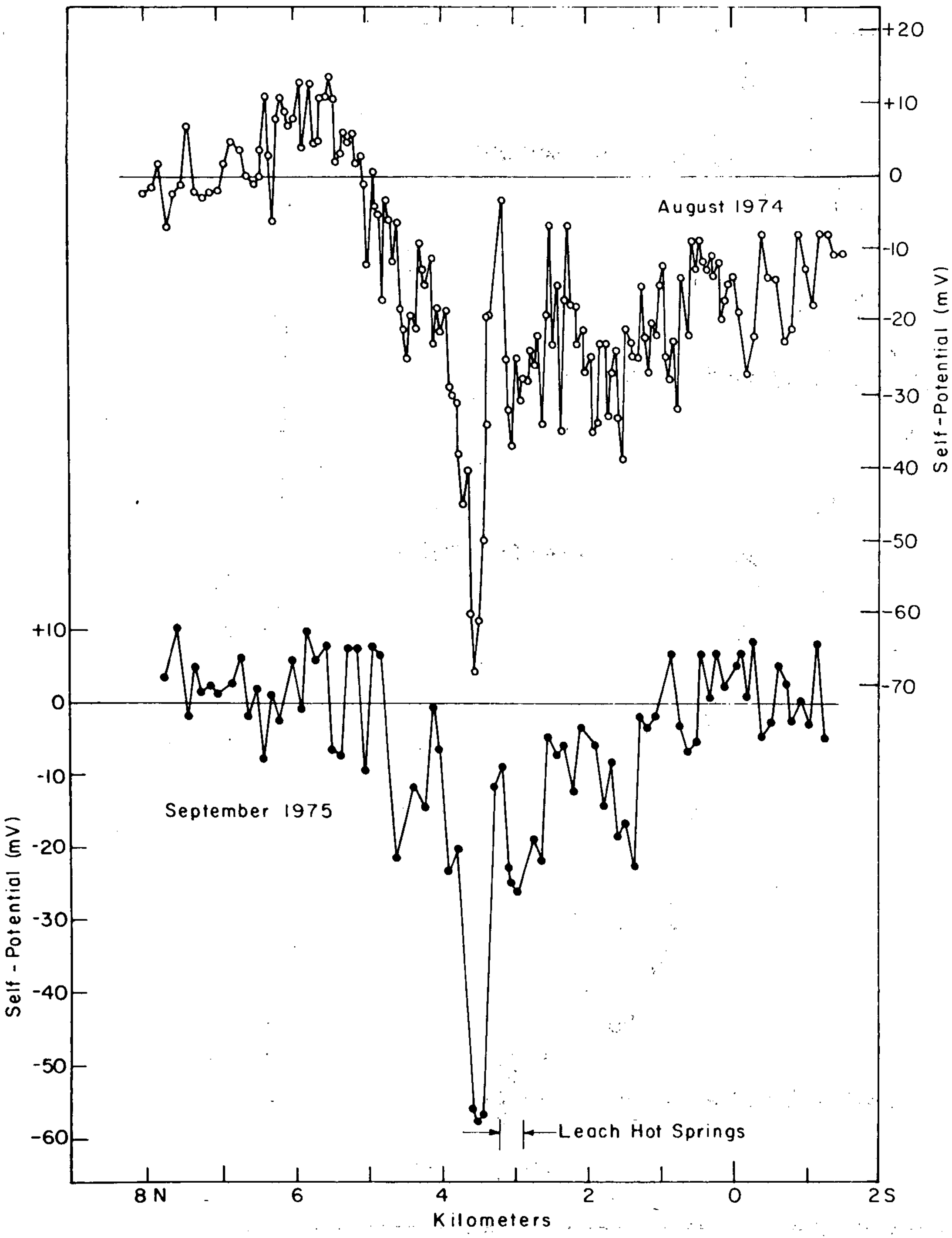

Figure 6

XBL 787-9596

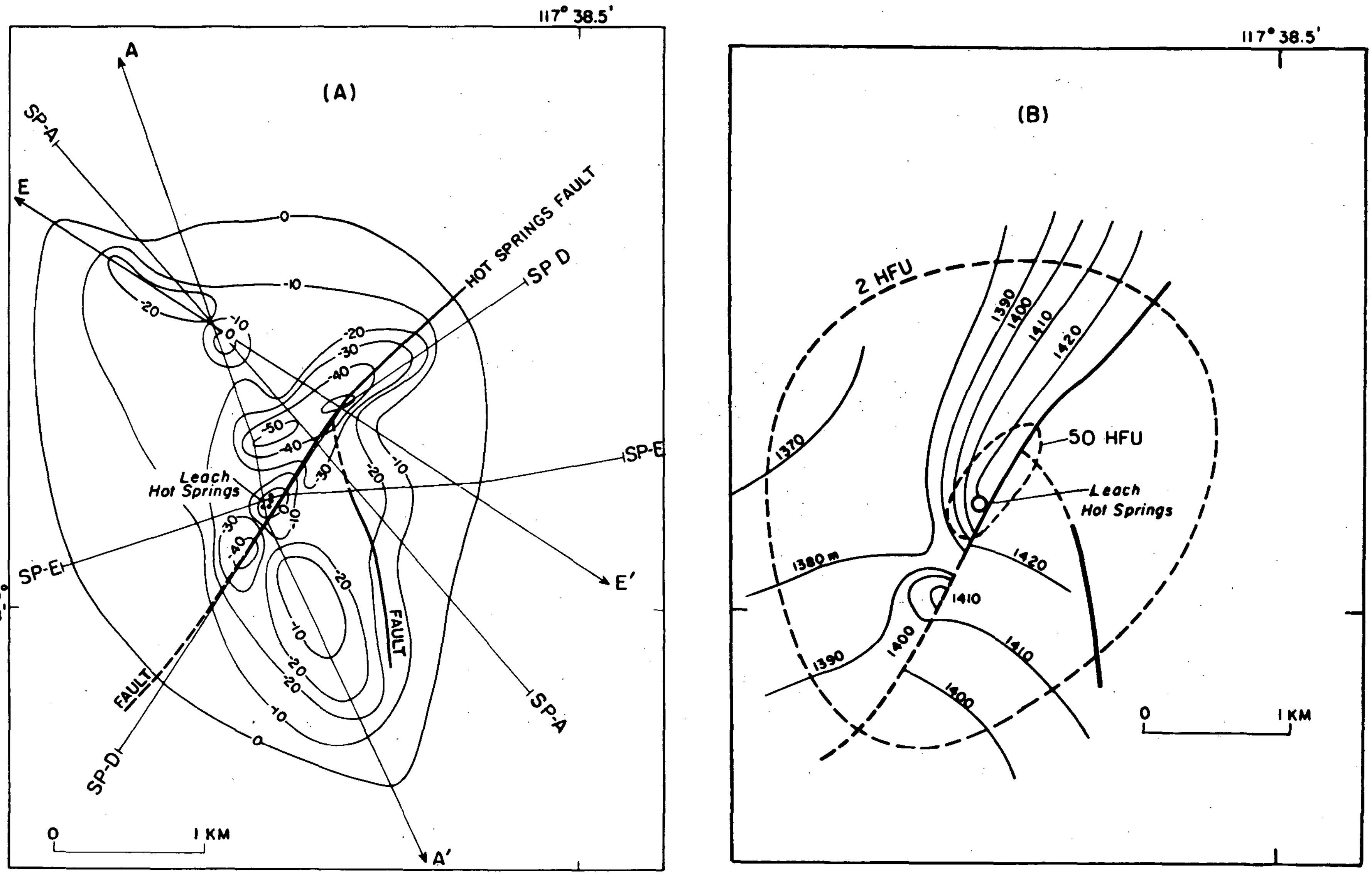

Figure 7

XBL 787-9599 A

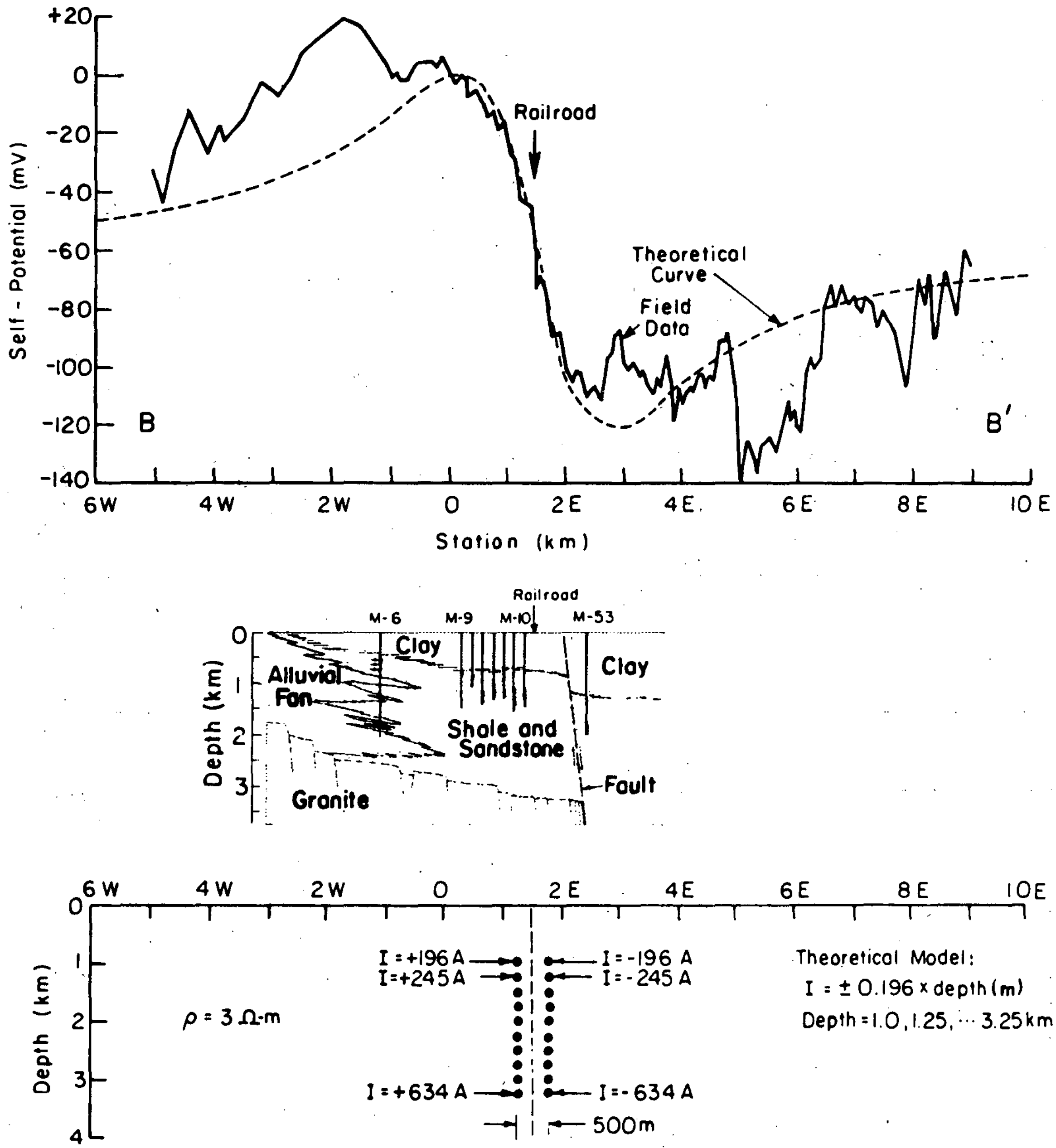

Figure 8

XBL 7?7-960C A

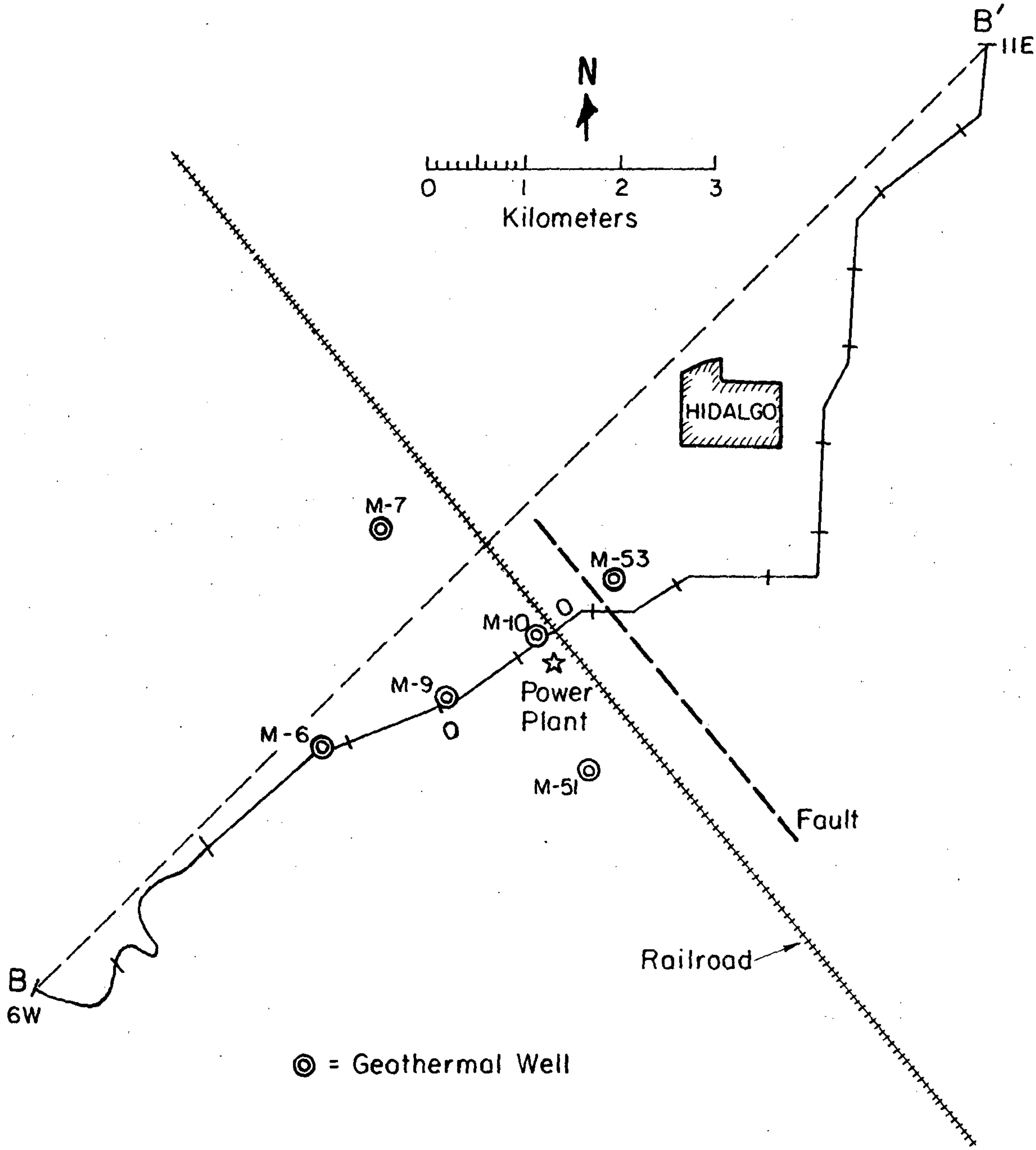

Figure 9

XBL 787-9593

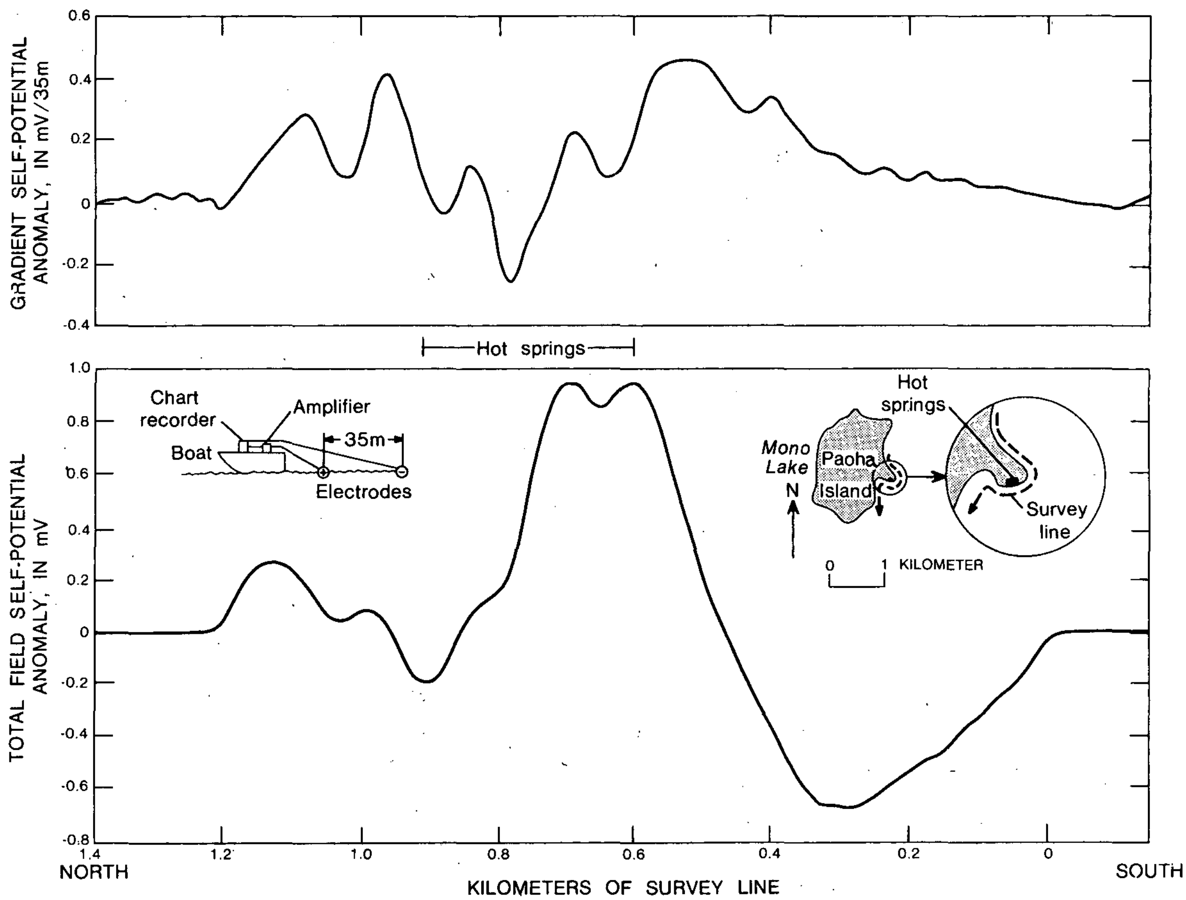

Figure 10

XBL 787-9601

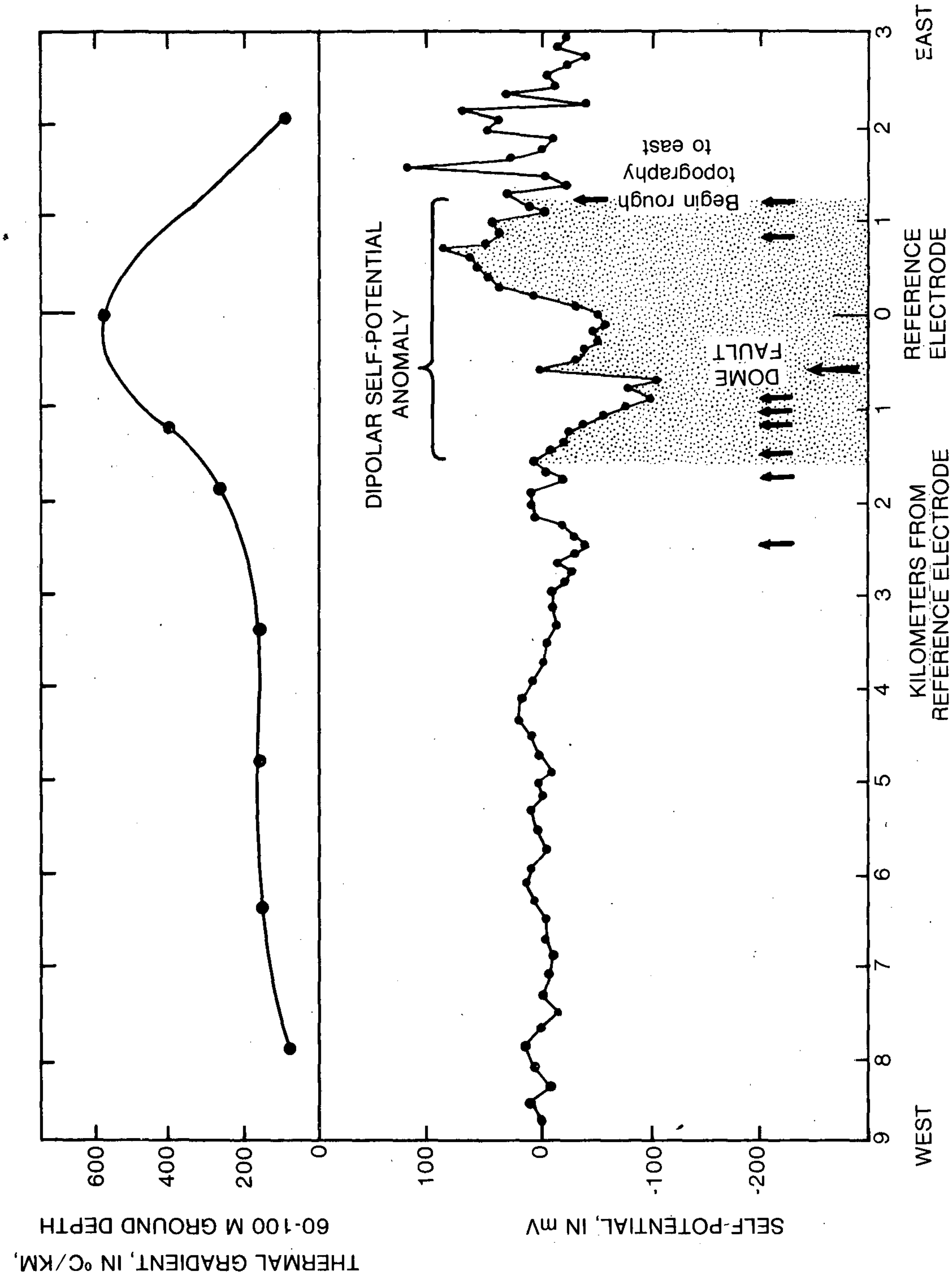

XBL 787-9602

Figure 11

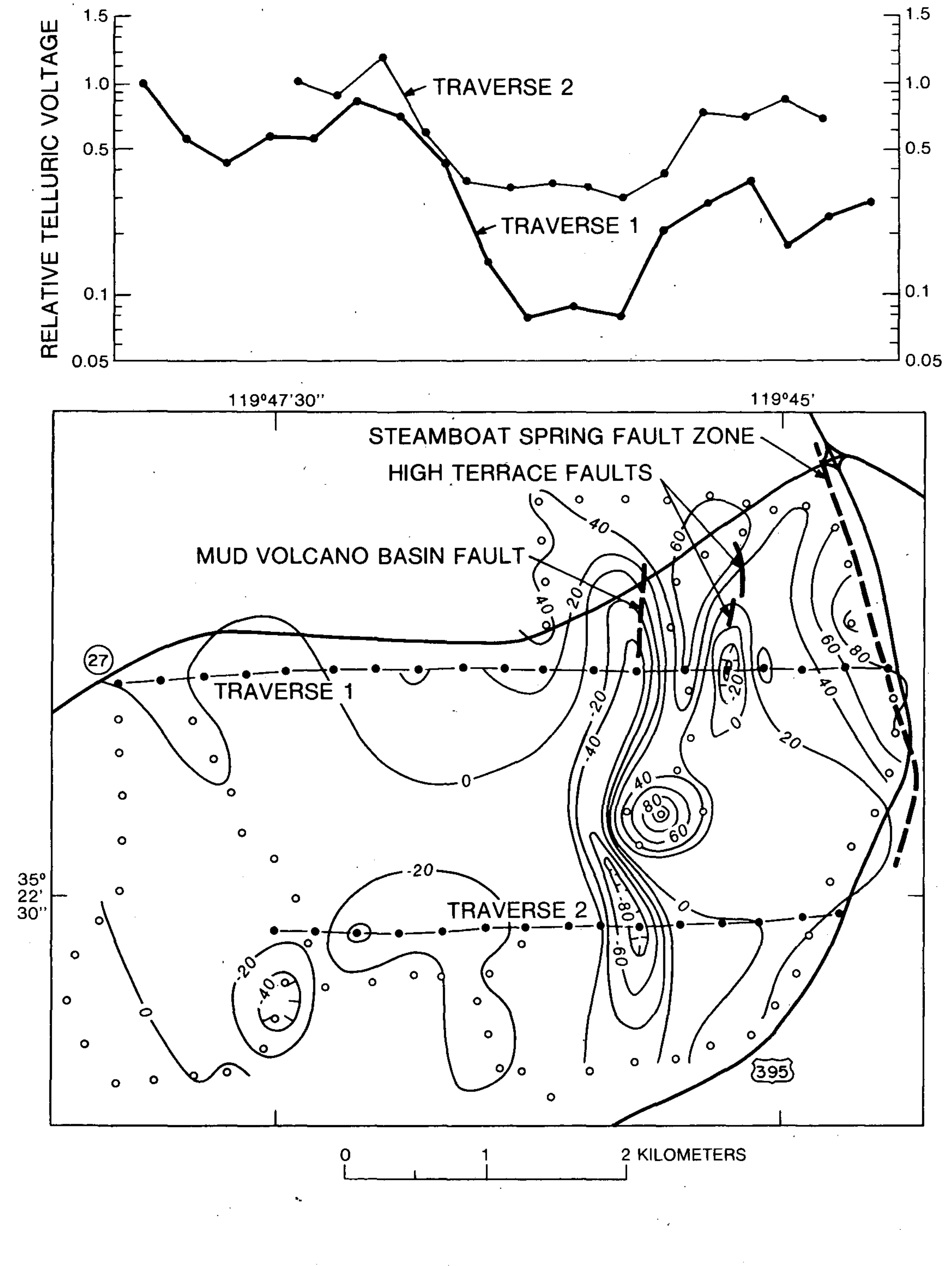

Figure 12

XBL 787-9603

TECHNICAL INFORMATION DEPARTMENT
LAWRENCE BERKELEY LABORATORY
UNIVERSITY OF CALIFORNIA
BERKELEY, CALIFORNIA 94720